Distribution of stratospheric column ozone (SCO) determined from satellite observations: Validation of solar backscattered ultraviolet (SBUV) measurements in support of the tropospheric ozone residual (TOR) method

Amy E. Wozniak,[1] Jack Fishman, Pi-Huan Wang,[2] and John K. Creilson[1]
NASA Langley Research Center, Hampton, Virginia, USA

Received 4 February 2005; revised 18 July 2005; accepted 27 July 2005; published 28 October 2005.

[1] The global (50°N–50°S) distribution of stratospheric column ozone (SCO) is derived using solar backscattered ultraviolet (SBUV) profiles and compared with SCO amounts derived from Stratospheric Aerosol and Gas Experiment (SAGE) and ground-based measurements. An evaluation of archived SBUV (version 6) ozone profiles with ozonesonde profiles shows that the low resolution of the SBUV instrument in the troposphere and lower stratosphere leads to a low bias in the SBUV profile in the troposphere and a high bias in the lower stratosphere in regions where anthropogenic tropospheric ozone production influences the climatology. An empirical correction applied to the SBUV profile prior to separating the stratosphere from the troposphere reduces the bias in the lower stratosphere and results in a SCO distribution in good agreement with SCO derived from SAGE ozone profiles. Because the empirical correction is most pronounced at northern middle latitudes, we compare these resultant SCO values with those measured at two northern middle latitude sites (Wallops Island and Hohenpeissenberg) using concurrent measurements from Dobson spectrophotometers and ozonesondes. Our analysis shows that the empirically corrected SCO at these sites captures the seasonal cycle of SCO as well as the seasonal cycle derived from SAGE stratospheric ozone profiles. These results have important implications for the derivation of tropospheric ozone from SBUV ozone profiles in conjunction with Total Ozone Mapping Spectrometer (TOMS) total ozone measurements using the tropospheric ozone residual (TOR) methodology.

Citation: Wozniak, A. E., J. Fishman, P.-H. Wang, and J. K. Creilson (2005), Distribution of stratospheric column ozone (SCO) determined from satellite observations: Validation of solar backscattered ultraviolet (SBUV) measurements in support of the tropospheric ozone residual (TOR) method, *J. Geophys. Res.*, *110*, D20305, doi:10.1029/2005JD005842.

1. Introduction

[2] Determination of the global distribution of tropospheric ozone is central to gaining a fundamental understanding of tropospheric chemistry and to assessing how human activity has perturbed the composition of the preindustrial atmosphere [e.g., see *Crutzen*, 1974; *Fishman and Crutzen*, 1978]. Attempts to produce a global distribution were first described in a series of studies in the 1970's using data from surface stations [*Fabian and Pruchniewicz*, 1973, 1977] and subsequently from analyses of ozonesonde measurements [*Chatfield and Harrison*, 1977; *Fishman et al.*, 1979]. Because of the variability inherently present in its distribution and abundance of tropospheric ozone, *Prinn* [1988] recognized the difficulty in obtaining a representative depiction by using only surface and ozonesonde measurements and suggested that a considerable international effort be initiated to derive an accurate global picture using conventional in situ measurement techniques. Although some progress has been made through the establishment of a number of ozonesonde stations at low latitudes through the SHADOZ (Southern Hemisphere Additional Ozonesondes) network [*Thompson et al.*, 2003], many regions on the planet remain significantly undersampled.

[3] In addition, an alternative approach to derive a global picture of tropospheric ozone using satellite information was introduced by *Fishman et al.* [1990] using concurrent observations of total ozone and a stratospheric ozone profile from independent satellite instruments to derive a quantity called the tropospheric ozone residual (TOR). Although the TOR did not yield any information about the vertical distribution of ozone within the troposphere, it did provide unique insight into the latitudinal, longitudinal and seasonal variability of the column abundance of tropospheric ozone.

[1] Also at Science Applications International Corporation (SAIC), Hampton, Virginia, USA.
[2] Also at Science and Technology Corporation, Hampton, Virginia, USA.

0148-0227/05/2005JD005842$09.00

[4] Global data sets of atmospheric trace gases using satellite observations have been primarily constrained to distributions in the stratosphere [*Kaye and Fishman*, 2003] since making measurements at these relatively higher altitudes is much simpler than in the troposphere. Validation of these stratospheric data products has been critical to the assessment of stratospheric ozone depletion and a monumental amount of research has been conducted to assess the accuracy of stratospheric ozone derived from satellites as well as determining how well various satellite techniques compare to one another [*World Meteorological Organization (WMO)*, 1999, 2003]. Thus we describe how relatively abundant stratospheric ozone profiles from satellite instruments such as SAGE (Stratospheric Aerosol and Gas Experiment) and SBUV (Solar Backscattered Ultraviolet) have been used to derive global TOR distributions, and then, as an alternative to explicitly validating the global TOR distribution, we assess the other component that comes out of TOR derivation, namely the global distribution of stratospheric column ozone (SCO). In the following sections we describe the methodology for deriving SCO from SBUV measurements, and validate the SBUV SCO through a comparison with SCO derived from SAGE measurements and with a comparable SCO quantity derived from concurrent ozonesonde and ground-based total ozone measurements.

2. TOR Method

[5] The first TOR method described by *Fishman et al.* [1990] used concurrent observations of total ozone from TOMS (Total Ozone Mapping Spectrometer) and stratospheric ozone profiles from SAGE to generate climatological maps of tropospheric column ozone. These depictions provided insight into how the seasonal tropospheric ozone distribution was influenced on hemispheric spatial scales by biomass burning in southern Africa and South America in the Southern Hemisphere, and by anthropogenic pollution sources from North America and Europe [*Fishman et al.*, 1990] in the Northern Hemisphere. Whereas using TOMS and stratospheric ozone profile data from SAGE and SAGE II archives could generate climatological TOR maps, generation of TOR fields with better temporal resolution requires a higher sampling frequency than the 30 daily occultations available from the SAGE instruments [*Vukovich et al.*, 1996]. The 40-day period required by SAGE to acquire pole-to-pole coverage precludes the possibility for deriving synoptic pictures on shorter timescales.

[6] The eruption of Mount Pinatubo in June 1991 prohibited the SAGE instrument from making accurate measurements in the lower stratosphere because of abnormally heavy aerosol loading, and thus TOR fields generated using concurrent measurements from TOMS and SBUV were derived for comparison with field measurements from NASA's 1992 Transport and Atmospheric Chemistry near the Equator-Atlantic (TRACE-A) mission [*Fishman et al.*, 1996b], a field campaign motivated by the first TOMS/SAGE TOR findings of elevated ozone over the tropical South Atlantic Ocean [*Fishman et al.*, 1996a]. The advantage of using SBUV data to derive stratospheric information for generating daily TOR fields is the global coverage (700–800 profiles daily) provided by the instrument. On the other hand, the vertical resolution of the SBUV measurement below the ozone peak is less than that of the SAGE instrument, and this method has been shown to have significant shortcomings when archived (version 6) SBUV data are used [*Vukovich et al.*, 1997; *Ziemke at al.*, 1998].

[7] Because of these noted shortcomings in the archived SBUV data, *Fishman and Balok* [1999] modified the archived SBUV profiles in the lower atmosphere by applying an "empirical correction" to the lowest three layers of the profiles. The Fishman and Balok study focused on the regional distribution of tropospheric ozone over the eastern United States and used ozonesonde information from Wallops Island (Virginia) to apply "corrections" to every archived SBUV profile used in the study. The empirical correction technique was then expanded from a regional to near-global domain (50°N to 50°S) in the work by *Fishman et al.* [2003] where the analyses derived by *Logan* [1999] were used to modify the archived SBUV profiles. It should be noted that the Logan tropospheric ozone climatology uses the global ozonesonde database as the primary input to drive her analysis. The resultant TOR distribution derived from TOMS and empirically corrected version 6 SBUV profiles (EC-TOR) made it possible to identify tropospheric regional scale ozone enhancements over a number of highly polluted regions (e.g., eastern United States, northern India, central Brazil, western Africa and central China).

[8] Subsequent to our use of the empirical correction to generate the TOR fields discussed by *Fishman et al.* [2003] and the SCO fields that will be discussed in the following sections, NOAA released a new archived SBUV data set (version 8). The primary improvement in the version 8 algorithm is an updated a priori ozone profile climatology. Whereas the old climatology was based on three latitude zones (low, middle, and high) and total ozone amount, the new ozone profile climatology divides profiles into 10° latitude zones (90°S to 90°N), altitude, and monthly averages. The new climatology also incorporates an updated balloonsonde climatology (1988–2002) in the troposphere and lower stratosphere, and SAGE II and MLS data in the middle and upper stratosphere [*McPeters et al.*, 2003]. A comparison of version 8 and version 6 profiles used in this study is presented in Appendix A.

3. Validation of the TOR Method and Purpose of this Study

[9] Since *Fishman et al.* [1990], there have been a number of studies that have used variations of the original TOMS/SAGE approach [*Ziemke et al.*, 1998; *Hudson and Thompson*, 1998; *Newchurch et al.*, 2001, 2003]. Each technique uses TOMS measurements to derive total column ozone and an additional measurement to define the stratospheric component of the total column to determine tropospheric ozone. The recent commentary by *deLaat and Aben* [2003] and the subsequent discussion by *Fishman* [2003] highlight the difficulty of validating TOR data against currently available databases. Validation of its near-global distribution without space-based measurements of similar resolution is extremely difficult and requires the continual deployment of near-earth instruments capable of measuring ozone columns throughout the entire troposphere (i.e., ozonesondes, aircraft profiles and UV-DIAL lidar measure-

Table 1. Definition of SBUV Ozone Profile Layers

SBUV Layer	Pressure Range, hPa	Midpoint Pressure, hPa	Approximate Midpoint Altitude, km
1	253–1013	507	5.5
2	127–253	179	12.5
3	63.3–127	89.6	17.0
4	31.7–63.3	44.8	21.3
5	15.8–31.7	22.4	25.8
6	7.92–15.8	11.2	30.4
7	3.96–7.92	5.60	35.2
8	1.98–3.96	2.80	40.2
9	0.99–1.98	1.40	45.4
10	0.495–0.099	0.700	51.0
11	0.247–0.495	0.350	56.5
12	0.0–0.2467	...	...

ments [see *Fishman et al.*, 1996a, 1996b]). *Sun* [2002] presented an excellent discussion on the accuracy of the TOR method when compared to ozonesonde measurements, and he has provided an analysis to show how each method varies with one another. He concludes that each of the six methods displays comparable differences with data from tropical ozonesonde stations (the region of interest in his study). Although each of the techniques was able to discern higher values over the Atlantic than over the Pacific, Sun noted that all the methods tend to underestimate the amount of ozone over the Atlantic. The study goes on to conclude that all TOMS-based methods seem to capture the variance better than the absolute amount. The accuracy of the empirical correction technique of *Fishman et al.* [2003], the focus of this study, was not included as part of the comparison by *Sun* [2002].

[10] Subsequently, *deLaat and Aben* [2003] questioned the accuracy of the EC-TOR fields presented by *Fishman et al.* [2003] and the finding of the regional nature of enhanced tropospheric ozone amounts at subtropical and northern middle-latitude locations. As pointed out by *Fishman* [2003], validation of TOR fields is extremely difficult without intensive dedicated field missions. On the other hand, the other product generated by the EC-TOR, namely the SCO, can be compared against available measurements derived from both in situ and satellite techniques. In turn, these satellite measurements have undergone intensive scrutiny since they have been used to assess how much ozone has been destroyed owing to the release of chlorofluorocarbons [*WMO*, 1999, 2003]. Since EC-TOR uniquely provides a long-term data set at middle latitudes in addition to low latitudes (the limitations of other TOR techniques) a more robust comparison can be performed because of the much larger set of measurements (i.e., including NH midlatitude ozonesonde/ground-based sites) against which the EC-TOR can be compared. *Fishman and Balok* [1999] show that the EC-TOR agreed much better with ozonesonde data than the TOR using archived SBUV data. In the following sections, we additionally will show how the empirical correction to the SBUV archive has improved the accuracy of the SCO derived from the EC-TOR methodology.

4. Methodology for Deriving Stratospheric Column Ozone From SBUV Profiles

[11] A challenge of using SBUV ozone profiles to derive stratospheric column ozone is in determining how to separate the troposphere from the stratosphere given the low resolution of the UV backscatter technique below the ozone peak. The following sections evaluate the dependence of the final profile on the a priori first-guess profile, compare the SBUV final solution profiles and ozonesonde measurements, and describe the empirical correction and its impact on the ozone profiles in the troposphere and lower stratosphere.

4.1. Ozone Profile Data

4.1.1. SBUV Ozone Profiles

[12] The SBUV instrument measures backscattered ultraviolet radiation at 12 different wavelengths to determine total ozone and the vertical ozone profiles. The SBUV instrument was launched on the NASA Nimbus-7 satellite and made measurements from November 1978 through June 1990. A similar record exists from January 1989 through the present from a slightly modified SBUV/2 instrument orbiting on the NOAA-11 satellite. The polar orbiting satellite platform provides global coverage every 6 days. The SBUV data used in the study were derived using the version 6 inversion algorithm and archived as profile layer amounts (see Table 1). Details of the version 6 retrieval algorithm and an error analysis of the SBUV ozone profiles are given by *Bhartia et al.* [1996].

4.1.2. Ozonesonde Profile Measurements

[13] The ozonesonde data used in this study were obtained from the ozonesonde database maintained by NASA Langley Research Center (V. Brackett, NASA Langley Research Center, personal communication, 2004). Stations chosen for comparison are between 50°N and 50°S (see Table 2) and have recurrent ozonesonde measurements from 1979 through 2000: Hohenpeissenberg, Sapporo, Sofia, Boulder, Wallops Island, Tateno, Kagoshima and Naha at northern midlatitudes; Nairobi and Natal at low latitudes; and Irene and Lauder at southern midlatitudes. A detailed description of the station data and the associated measurement error are presented by *Logan* [1999].

4.2. Comparison of Archived SBUV Ozone Profiles With the A Priori First-Guess Profiles in the Troposphere

[14] The UV wavelengths used to determine the ozone profile in the troposphere and lower stratosphere are sensitive to aerosols, clouds and ozone over a broad range of altitudes. Such sensitivities limit the vertical resolution of the instrument to approximately 15 km below the peak, whereas the resolution above the peak is approximately

Table 2. Individual Stations With Ozonesonde and Ground-Based Total Ozone Measurements

WMO ID	Station Name	Latitude, deg	Longitude, deg
099	Hohenpeissenberg, Germany	47.80 N	11.02 E
012	Sapporo, Japan	43.05 N	141.33 E
132	Sofia, Bulgaria	42.81 N	23.38 E
067	Boulder, Colorado	40.03 N	105.25 W
014	Tateno, Japan	36.05 N	140.13 E
107	Wallops Island, Virginia	37.93 N	75.48 W
007	Kagoshima, Japan	31.55 N	130.55 E
190	Naha, Japan	26.20 N	127.68 E
175	Nairobi, Kenya	1.27 S	36.80 E
219	Natal, Brazil	5.42 S	35.38 W
265	Irene, Pretoria, South Africa	25.90 S	28.22 E
256	Lauder, New Zealand	45.03 S	169.68 E

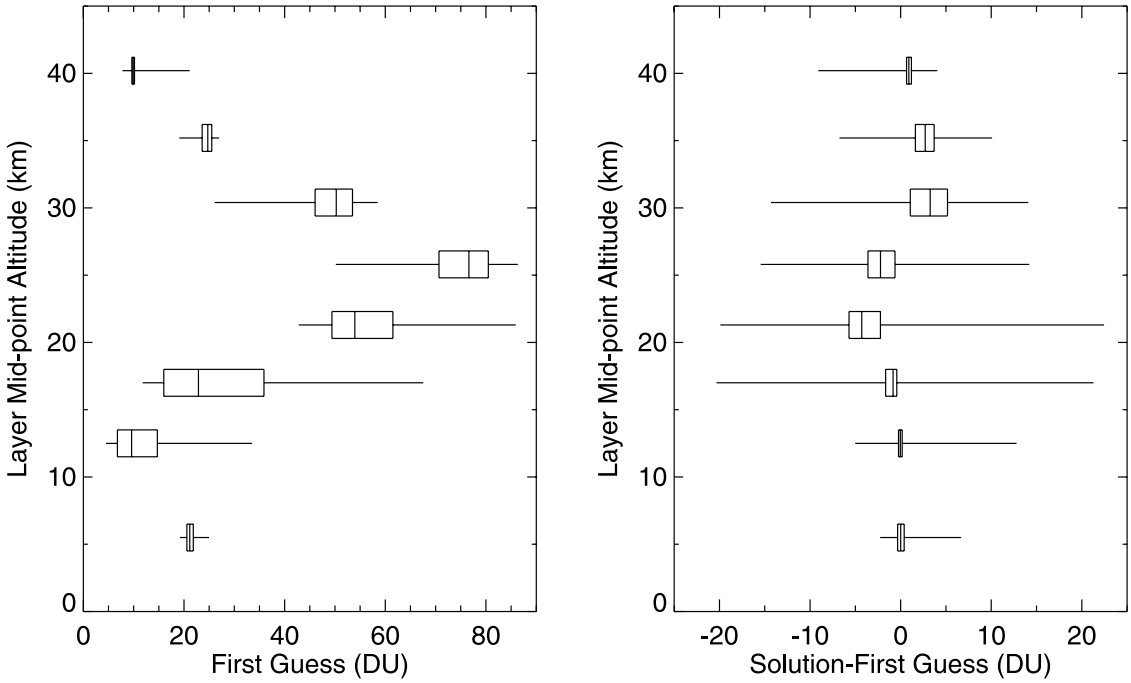

Figure 1. (left) A box-and-whiskers plot of the NOAA-11 1999 50°S to 50°N first-guess profile layers as a function of layer midpoint altitude. The left and right edges of the box show the lower and upper quartiles, respectively. The line through the middle of the box shows the median value and the whiskers show the minimum and maximum values for each layer. (right) A box-and-whiskers plot for the difference between the final solution profile and first-guess profile (final solution-first guess) for each layer.

8 km. The decreased sensitivity to ozone in the lower portion of the profile forces the retrieval algorithm to depend heavily on the a priori first-guess profile shape and the total ozone amount in determining the final profile below the ozone peak [*McPeters et al.*, 1986]. The version 6 SBUV retrieval a priori first-guess profiles are classified by total ozone and latitude and derived from SAGE and ozonesonde profiles. Figure 1 shows a box-and-whisker plot of the NOAA-11 1999 50°S to 50°N first-guess ozone profile layers (Figure 1, left) and the difference between the final solution profile and first-guess profile for each layer (Figure 1, right). The graphs show data from over 200,000 profiles. The left and right edges of the box are the upper and lower quartiles of the difference and the line through the middle of the box is the mean. The whiskers extend to the minimum and maximum values. Figure 1 shows that the first-guess Layer 1 has the least variable climatology below the ozone peak and that the majority of the variability in the profile shape, and therefore total column ozone, comes from Layers 2 through 6. It is clear from Figure 1 (left) that the first-guess value of Layer 1 ranges from approximately 20 DU to 25 DU and from Figure 1 (right) that the range of the final solution profile is within −2 DU to +6 DU of the first-guess value with a most probable value of zero. We will show in the following comparison of SBUV profiles with ozonesonde profiles that owing to the limited a priori first-guess climatology, the Layer 1 final solution is generally lower than the climatological ozonesonde value and also lacks the seasonal variability seen in the in situ measurements [e.g., see *Fishman and Balok*, 1999, Plates 1 and 2]. Conversely, the final solution to Layer 3 is nearly always higher than that of the ozonesonde values.

4.3. Comparison of SBUV Ozone Profiles With Ozonesonde Measurements in the Troposphere and Lower Stratosphere

[15] The following results are quantitative comparisons of the combined 16-year Nimbus-7 and NOAA-11 archived version 6 SBUV ozone profile data set with an ozonesonde profile data set consisting of more than 3000 measurements from 12 stations at middle to low latitudes. The high-resolution ozone soundings were integrated to obtain the layers defined in Table 1. SBUV profile measurements were required to be within 5° latitude by 5° longitude of the ozonesonde station location and on the same day as the ozonesonde launch. The comparison focuses on Layers 1 through 5 since most ozonesondes burst before reaching 15.8 hPa. Layer 1 represents the amount of ozone in the troposphere. Layers 2 and 3, depending on latitude and tropopause height, can be a mix of tropospheric and stratospheric air. Layers 4 and 5 are representative of stratospheric concentrations at the ozone profile maximum.

[16] Figure 2 shows the mean difference (SBUV-Ozonesonde) and standard deviation of the SBUV layer amounts compared with ozonesonde measurements. Positive differences indicate SBUV is overestimating the amount of ozone in the layer, and negative differences indicate SBUV is underestimating the amount of ozone in the layer. In the previous section we determined that there is little if any change in Layer 1 ozone from the first-guess climatology to

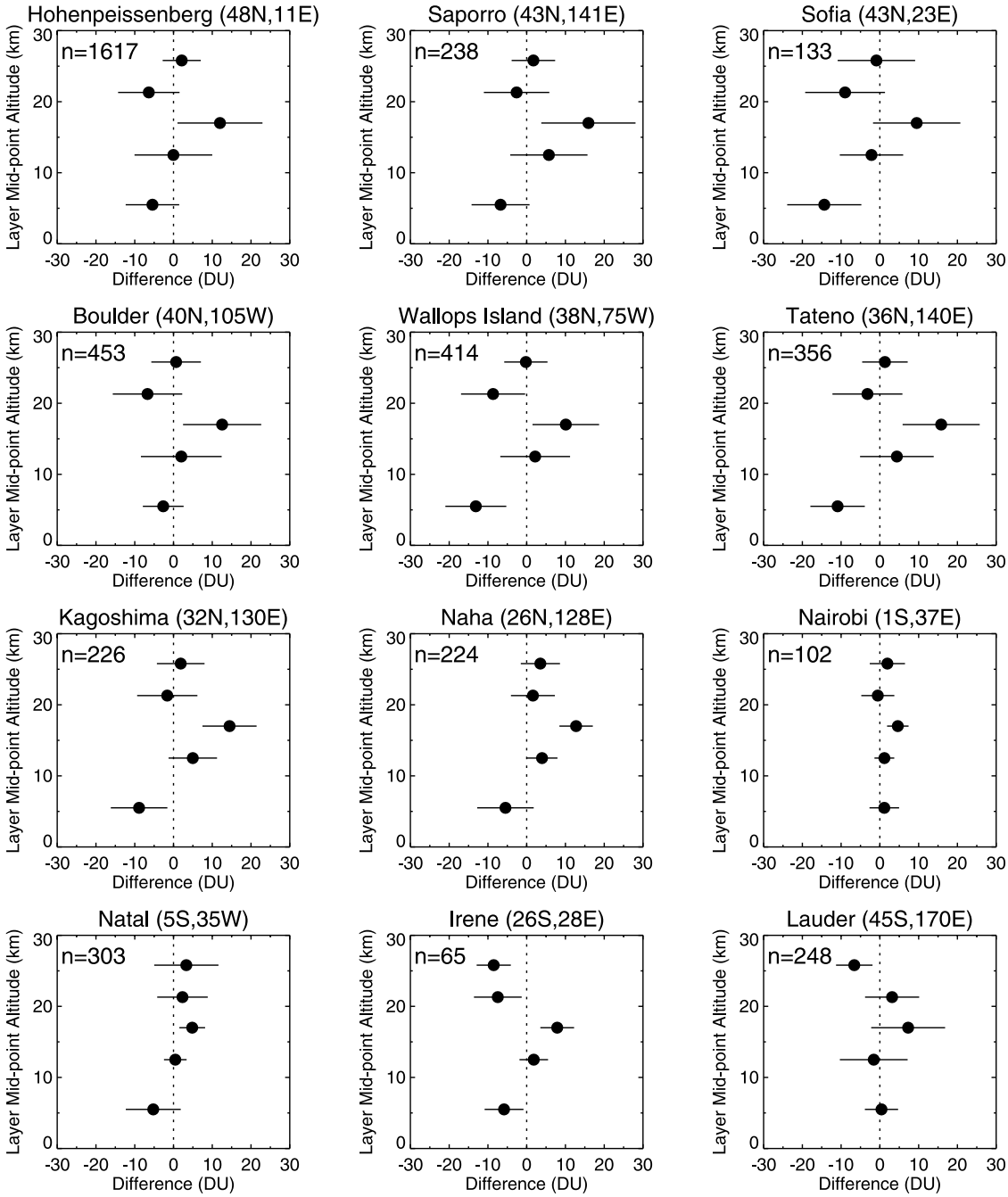

Figure 2. Mean difference (SBUV-Ozonesonde) for archived version 6 SBUV Layers 1 through 5 when compared with ozonesonde profiles. The solid bars represent 1-sigma standard deviation from the mean.

the final solution profile, therefore differences in SBUV and ozonesonde values can be directly attributed to the first-guess climatology. At 10 of the 12 ozonesonde stations used in the comparison, the amount of ozone in SBUV Layer 1 is less then the amount of ozone in the ozonesonde Layer 1 and conversely, the amount in ozone in SBUV Layer 3 is greater than the amount of ozone in the ozonesonde Layer 3. Given that the integral of the lowest 3 Layers is a truer representation of the vertical resolution of the instrument, Figure 2 suggests that excess ozone below the ozone peak is erroneously placed in Layer 3 owing to the invariant Layer 1 first-guess climatology.

[17] Tropospheric ozone production increases in the Northern Hemisphere during the summer months (JJA) owing to photochemical production associated with anthropogenic emissions of NO_x and CO [*Wang et al.*, 1998]. The seasonal nature of excess tropospheric ozone production should produce a seasonal trend in the mean difference between the Layer 1 and Layer 3 SBUV ozone and comparable ozonesonde amounts. Figure 3 shows the monthly mean differences of SBUV Layer 1 and Layer 3 ozone amounts compared with ozonesonde values (SBUV-Ozonesonde). At the midlatitude Northern Hemisphere stations of Hohenpeissenberg (48°N), Saporro (43°N), Sofia

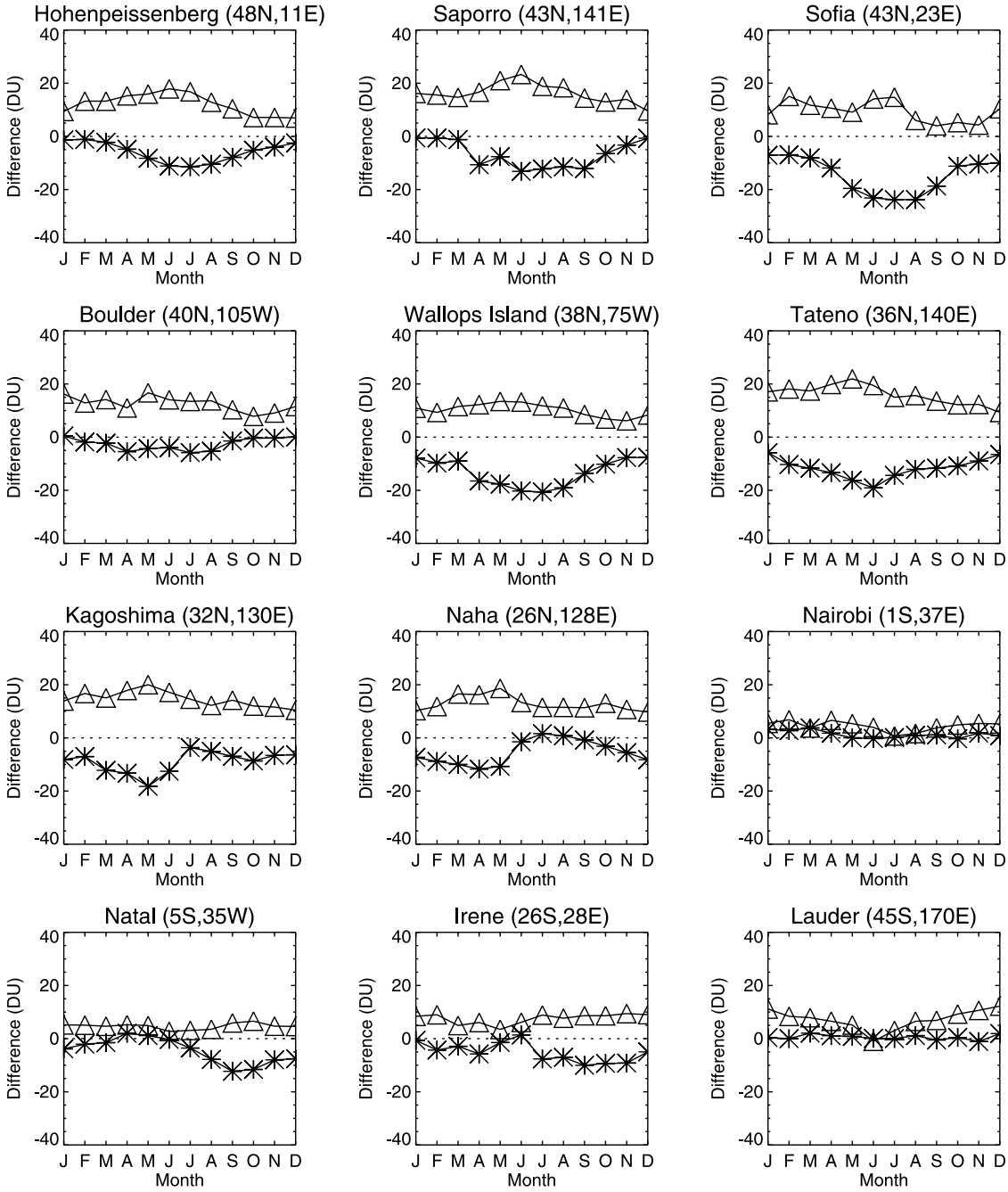

Figure 3. Monthly mean differences between of SBUV profiles and ozonesonde profiles (SBUV-ozonesonde) in Layer 1 (asterisks) and Layer 3 (triangles).

(43°N), Boulder (40°N), Wallops Island (38°N), and Tateno (36°N), the difference between the satellite and ozonesonde measurements of Layer 1 are greatest during the June, July and August (JJA) summertime ozone maximum. This seasonal mean difference between SBUV and ozonesondes in Layer 1 is less pronounced at Boulder than the other midlatitude Northern Hemisphere stations owing to its high-altitude location. The Boulder station is located 1634 m above sea level which will bias the ozonesonde integral between 1013 hPa and 253 hPa (Layer 1) low compared to the other stations at similar latitude.

[18] In contrast to the higher latitude Japanese stations of Saporro and Tateno, lower latitude stations Kagoshima (32°N) and Naha (26°N) show the mean difference in Layer 1 is a maximum during the spring in May and minimum during the summer in July. Layer 3 shows similar seasonal behavior. These stations have a maximum in ozone in spring, which coincides with increased photochemical production of ozone. The sharp decline in the difference in June and July is due to the summer monsoon pattern of low ozone air from the tropical Pacific being advected onto the island [*Logan*, 1985, 1999].

[19] At the two South Atlantic stations of Natal (5°S) and Irene (26°S), maximum mean differences are shifted into austral spring (September–November), coincident with the peak of biomass burning. South American and African

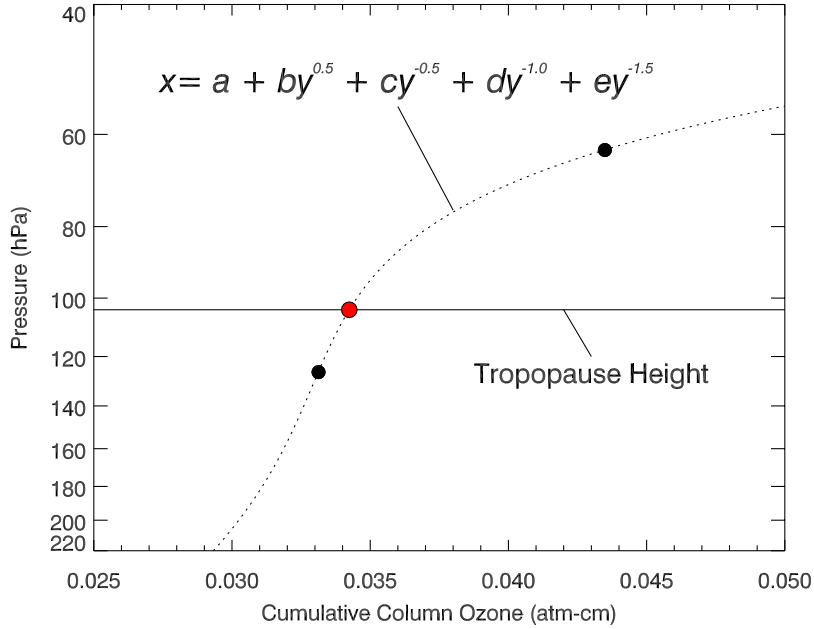

Figure 4. Interpolation of the cumulative SBUV ozone to the tropopause pressure using a fifth-order polynomial. The solid black circles represent the cumulative SBUV ozone at the top of Layers 2 and 3. The solid red circle represents the interpolated cumulative amount of ozone at the tropopause pressure using the fifth-order polynomial.

biomass burning, respectively, influence Natal and Irene. Irene is another station, like Boulder, with a low bias in Layer 1 compared with other stations at the same latitude because the site is 1523 m above sea level. Irene is influenced by African biomass burning in austral spring and year-round by anthropogenic emissions from Pretoria and Johannesburg [*Diab et al.*, 2004]. A strong seasonal correlation between ozone and CO measurements from MOPPIT exists at both locations [*Bremer et al.*, 2004].

[20] At the two Pacific stations of Nairobi (1°S) and Lauder (45°S), differences are close to zero in Layer 1 and show only slight differences in Layer 3. The Nairobi ozonesonde station is part of the SHADOZ network, and the tropospheric columns are lower than other SHADOZ stations that may be influenced by African biomass burning sources. *Thompson et al.* [2003] cite two possible reasons for this difference: First, high terrain removes approximately 3–5 DU of ozone since the elevation of the Nairobi station is 1795 m; second, Thompson et al. show, through 5-day back trajectories at 500 hPa, that Nairobi is influenced primarily by air masses with origins east of the continent over the Indian Ocean and not from air re-circulated over southern Africa. The ozonesonde station at Lauder exhibits minimal seasonal variability in tropospheric ozone and is in excellent agreement with the SBUV first-guess climatology in Layer 1. Layer 3 differences increase during Southern Hemisphere summer (DJF), consistent with previous findings when this layer was compared with profiles derived from SAGE at these latitudes [*McPeters et al.*, 1994].

4.4. Application of Empirical Correction to the SBUV Profiles

[21] We have shown that the amount of ozone in the lower stratosphere in SBUV Layer 3 from 127 hPa to 63 hPa is consistently overestimated when compared to the ozonesonde climatology and conversely, the lowest layer in the SBUV profile, Layer 1, from 1013 hPa to 253 hPa is consistently underestimated when compared with the ozone climatology at stations where excess photochemical production of ozone contributes significantly to the climatology. This finding prompted the use of an empirical correction to the SBUV profiles to reduce the seasonal bias in Layer 3 based on a monthly climatology developed by *Logan* [1999] and described by *Fishman et al.* [2003]. Since the final solution profile contains no information in the troposphere, we replace the SBUV Layer 1 and Layer 2 with the Logan climatology and apply the residual as a correction to the lower stratosphere (Layer 3). The tropospheric portion of the profile is prescribed as a function of geographic location and month of the year. It takes into account regional and seasonal tropospheric enhancements that were not included in the version 6 a priori first-guess ozone profiles, which were based solely on total ozone and latitude. The empirically corrected ozone profile is then integrated to the NCEP tropopause pressure. The tropopause pressure will vary according to global location and time of year and will generally lie within Layer 2 or Layer 3.

[22] An illustration of how the interpolation within Layer 3 is applied is shown in Figure 4. We have developed a fifth-order polynomial fit between Layer 2 and Layer 3 that predicts the cumulative amount of ozone as a function of pressure. Using the curve defined by the polynomial, the amount of integrated ozone below the tropopause is calculated using the NCEP tropopause height information. That quantity is then subtracted from the SBUV total ozone amount to define the SCO. The estimated error associated with the interpolation based on testing with over 11000 ozonesondes (not limited to the 12 stations used in this

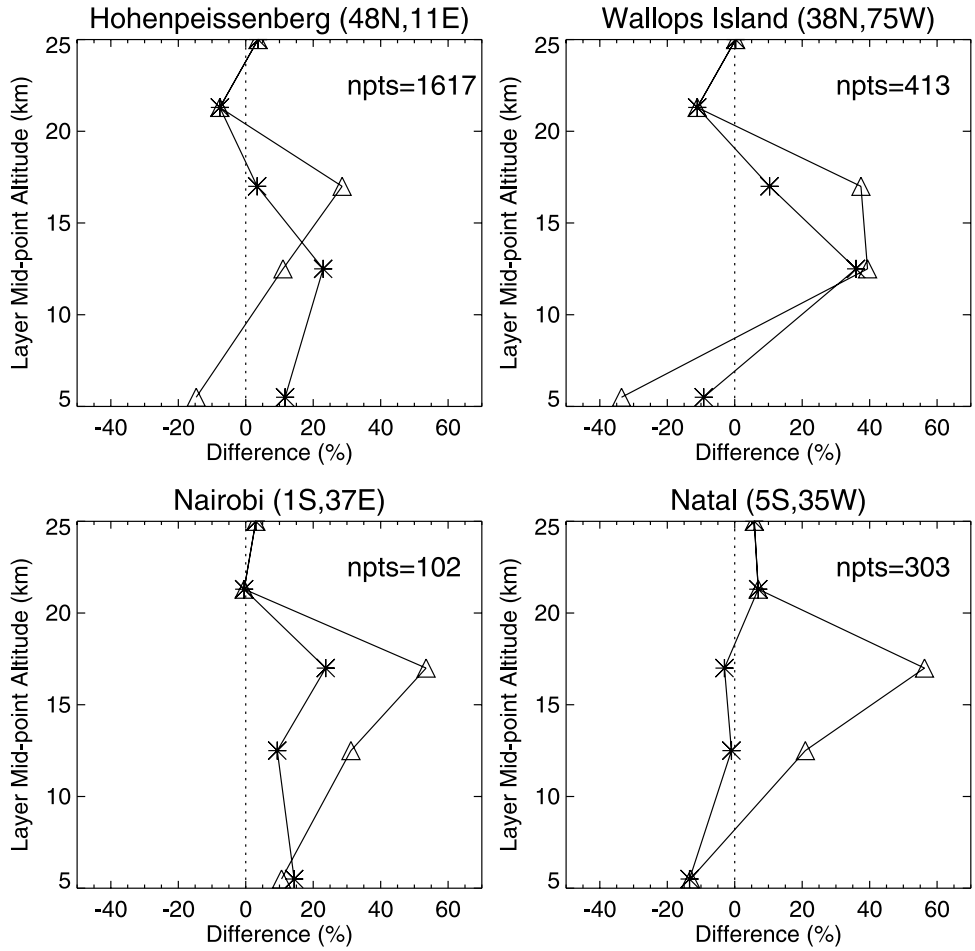

Figure 5. Mean bias of SBUV profiles compared with ozonesonde profiles (SBUV-ozonesonde/ozonesonde) for Layers 1–5 at four locations. Triangles are uncorrected SBUV profiles and asterisks and corrected SBUV profiles.

study) launched between 1996 and 2003 is 0 ± 2 DU. Figure 5 summarizes the mean difference between the archived and empirically corrected SBUV layers and corresponding ozonesonde layers for four stations ranging in latitude from 47°N to 5°S. The empirical correction has lowered the bias in Layer 3 at all stations.

[23] The residual methodology relies on each individual SBUV ozone profile measurement to compute the SCO and capture the large-scale synoptic patterns that define the stratospheric ozone distribution. By applying the empirical correction to the lowest three layers of the ozone profile we can improve calculation of the stratospheric column ozone by improving the retrieved ozone profile in the troposphere and lower stratosphere (Layers 1 through 3). It is possible that other perturbations in the profile radiances can cause the overestimation of the lower stratospheric layer, which would not be remedied through the application of the empirical correction. On the other hand, we can show that the resultant SCO distribution is an improvement over the SCO derived from archived SBUV profiles. The uniqueness of the SBUV record and the plans for continued SBUV instrument measurements encourages us to continue investigating the value of SBUV ozone profile measurements for determining stratospheric column ozone and its usefulness in the derivation of tropospheric ozone fields in conjunction with total column ozone from TOMS.

5. Validation of SBUV Derived Stratospheric Column Ozone

[24] Although satellite measurements provide much better temporal and spatial resolution than individual ground measurement stations, validation of the resultant satellite distributions is intrinsically challenging. Accurate measurements of the entire stratospheric column are difficult to achieve from any one instrument. Ground-based methods (e.g., lidar) can experience interference from atmospheric aerosols and pollution, or be limited in altitude range; similarly, satellite-based measurements typically lose accuracy at lower altitudes owing to radiative interference from multiple sources. Thus we have chosen two methods to test the validity of SBUV SCO data set: comparison against other independently derived quantities (as in the previous section) and a comparison with fields derived from another satellite data set which we know correctly captures the vertical structure throughout the stratosphere. For this latter portion of the validation study, we compare the EC-SBUV

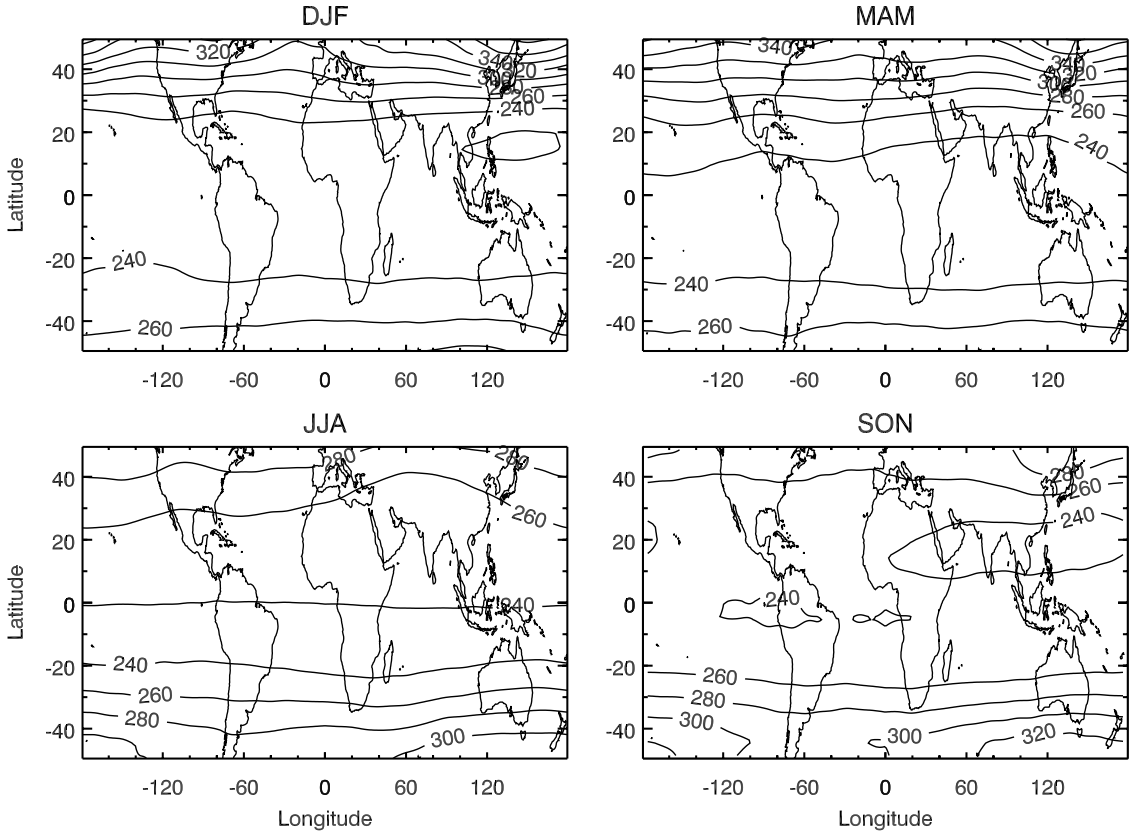

Figure 6. Seasonal stratospheric column ozone distribution derived from SAGE II (1985–2000) ozone profiles.

SCO with SCO fields derived from SAGE profiles. The results of this comparison are presented below.

5.1. Comparison of SBUV and SAGE Derived Stratospheric Column Ozone Fields

[25] Stratospheric ozone profile measurements made from SAGE II from 1985 through the present provide solar occultation measurements of ozone profiles with much higher vertical resolution than SBUV to derive stratospheric column ozone. The SAGE ozone profile measurements have been shown to be in agreement with ozonesonde measurements to within 10% down to the tropopause [*Wang et al.*, 2002].

[26] Figure 6 shows the seasonal stratospheric ozone climatology derived from integrating high vertical resolution SAGE II profiles above the NCEP tropopause height. Profile measurements from 1985 through 2000 were included except for those in the 3 years following the June 1991 eruption of Mount Pinatubo. The dynamical movement of the tropopause height is the primary determinant of the stratospheric ozone column. The strongest gradients are located in the vicinity of strong jet streams where strong gradients in tropopause heights can be found. Most of the ozone is located in the stratosphere, and the same gradients in Figure 6 SCO from SAGE II can also be observed in the total column ozone, particularly in the absence of chemical production in the troposphere. SCO is lower in the tropics owing to higher tropopause heights and therefore less mass in the stratosphere. Outside of the tropics, the tropopause height generally decreases toward the poles. Because the tropopause height is determined from the temperature profile, there are seasonal differences in the stratospheric ozone fields between hemispheres. In the summer hemisphere, stratospheric column ozone values are lower than in the winter hemisphere. Stratospheric column ozone values are larger in the Northern Hemisphere in winter (December through February) and spring (March through May), than during the summer (June through August) or fall (September through November) months. The same pattern is seen during the Southern Hemisphere winter and spring (JJA and SON) relative to austral summer and autumn (DJF and MAM). The variability of the position of the midlatitude jet stream and separation between tropical and midlatitude air masses results in the stratospheric ozone gradient becoming less zonal outside the tropics. The SCO minimum does not occur exactly at the equator, but rather at the low latitudes of the winter hemisphere.

[27] Figure 7 shows the seasonal stratospheric ozone columns derived from Nimbus-7 SBUV and NOAA-11 SBUV/2 empirically corrected ozone profiles from 1985 through 2000 integrated above the NCEP tropopause height. The SBUV seasonal climatologies show similar patterns of increasing ozone toward the poles, the seasonal shift of the minimum in the tropics, and the zonal asymmetry in the midlatitudes.

[28] Figure 8 shows the differences in Dobson Units between the SAGE and the EC-SBUV seasonal SCO climatologies superimposed on the 500-hPa horizontal (u) wind field. The solid contours indicate when EC-SBUV SCO is high compared to SAGE and dashed contours

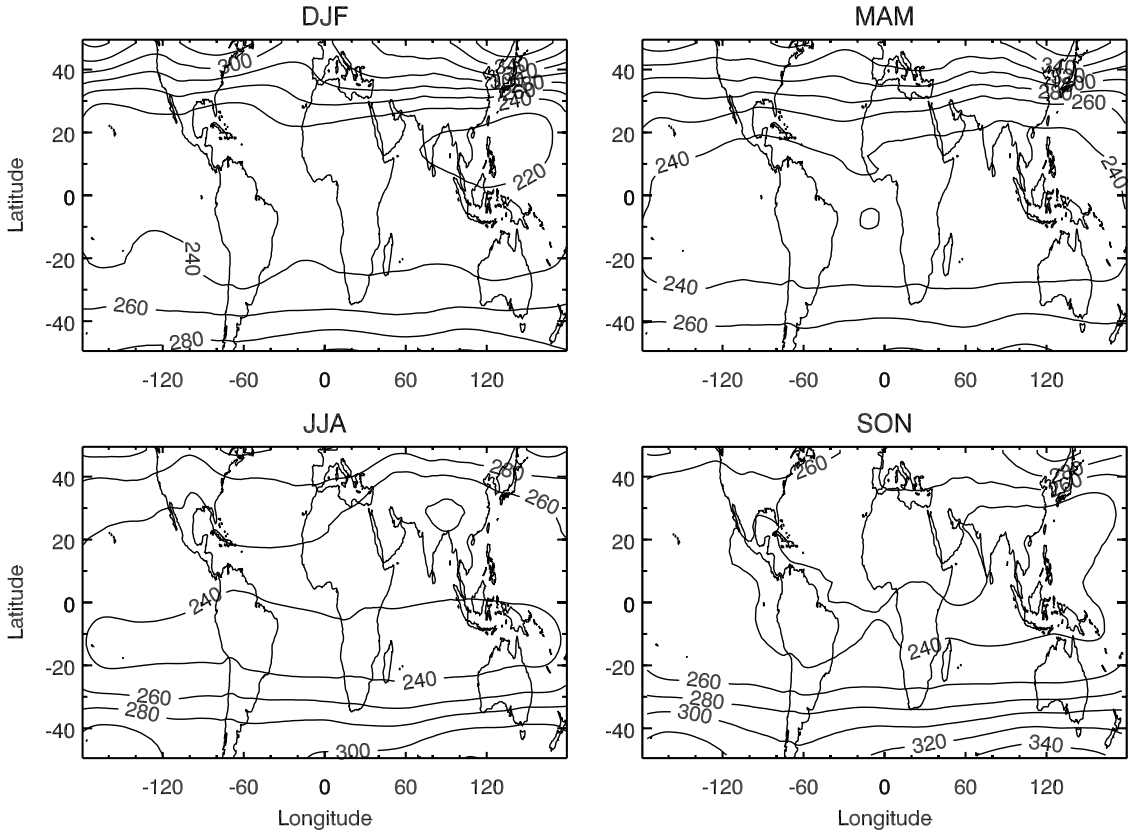

Figure 7. Same as Figure 6 except using data from empirically corrected SBUV measurements from 1985 through 2000.

indicate when EC-SBUV SCO is low compared to SAGE. The greatest absolute differences occur at latitudes greater than 40° in the Southern Hemisphere during SON and DFJ. These differences are consistent with comparisons of SAGE and SBUV that show SBUV greater than SAGE in the lower stratosphere by approximately 10% [*McPeters et al.*, 1994; *SPARC*, 1998]. Other significant differences are in the regions over the western Pacific Ocean east of the Asian continent, and over the northwestern Atlantic off of the east coast of the United States, and also south of Europe over Northern Africa and western Asia. These features are strongest in DJF and MAM, but generally persist throughout the year. These three large differences coincide with local maxima in the midlatitude jet stream.

[29] Figure 9 highlights improvement of the EC-SBUV SCO over the archived SBUV SCO relative to the SAGE SCO distribution (i.e., the quantity | SBUV – SAGE| – |EC-SBUV – SAGE|). Regions with positive values indicate where the EC-SBUV climatological value is now closer to the SAGE climatological value. Improvements of more than 5 DU are found over much of the Northern Hemisphere and over the South Atlantic off the coast of Southern Africa. The greatest improvement is over the Northern Hemisphere during the summer months (JJA). Regions of no improvement (negative values) are typically in the midlatitude storm tracks. Above the surface (1000 hPa) at northern midlatitudes (>20°N), the Logan climatology is zonally symmetric, and therefore will not reflect higher ozone amounts in the upper troposphere in regions where higher ozone amounts are present owing to enhanced outflow from the stratosphere [*Beekman et al.*, 1997].

5.2. Comparisons of SBUV Derived Stratospheric Column Ozone With In Situ and Ground-Based Measurements

[30] In this section we compare empirically corrected SBUV SCO with stratospheric columns derived from coincident ground-based total ozone measurements and integrated tropospheric column ozone from ozonesondes using the WMO definition of the thermal tropopause height for each sounding. The total ozone measurements used in this study (also see Table 2) were obtained from the World Ozone Data Center maintained by Environment Canada. The daily total column ozone values for all stations except Sofia, Bulgaria, were made with Dobson spectrometers. The daily total column ozone from Sofia, Bulgaria, was measured using a filter ozonometer. A discussion of the different methods and comparisons of the ground-based total ozone measurements with Nimbus-7 TOMS and SBUV measurements is provided by *Fioletov et al.* [1999].

[31] Figure 9 shows that the largest changes in SCO resulting from the empirical correction take place at Northern Hemisphere (NH) middle latitudes, especially in spring and summer. We compare satellite-derived SCO values with SCO integrals generated at the NH middle latitude ozonesonde sites of Hohenpeissenberg (47°N, 11°E) and Wallops Island (38°N, 75°W). For the data summarized in Tables 3a and 3b and Figures 10a and 10b, 1347 ground-based obser-

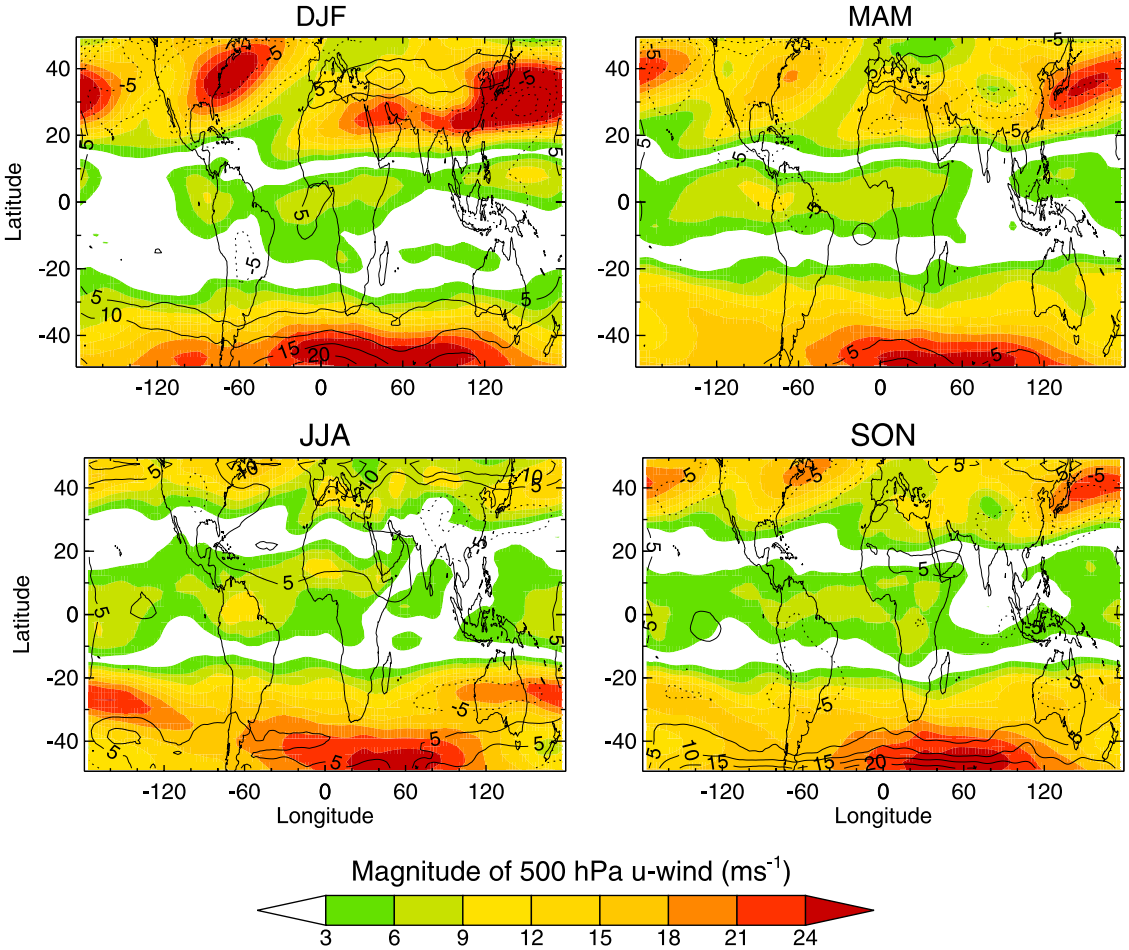

Figure 8. Solid and dashed contours depict the difference between EC-SBUV and SAGE (EC-SBUV − SAGE) stratospheric column ozone fields. The magnitude of the 500-hPa u-wind (m s^{-1}) is shown by the color contours.

vations were included in monthly averages at Hohenpeissenberg and 416 at Wallops Island. SAGE profiles that were within 1000 km of each of the two stations were used in the analysis, resulting in 1031 profiles at Hohenpeissenberg and 1488 profiles at Wallops Island. No coincident time criterion was imposed on the SAGE overpass and ozonesonde launch times, as this would have greatly diminished the number of profiles that could have been used to determine the monthly climatological values. Monthly SBUV values were calculated by averaging 17 years of daily SCO fields, interpolated to a 1.0° by 1.25° matrix, at the grid point closest to each of the ground station locations.

[32] *Wang et al.* [2002] performed a detailed comparison of coincident SAGE and ozonesonde profiles at Hohenpeissenberg. Examination of 329 coincident profiles (which in their study meant within 24 hours and within ∼1000 km) shows that there is excellent agreement between 13 and 28 km, with the middle latitude stations generally within 5% down to 20 km and within 10% down to 10 km. SAGE exhibits a positive bias between 15 and 20 km, which is consistent with our analysis, but the data presented in Table 3a and Figure 10a suggest that this bias is most pronounced in November and December, the only 2 months where the SAGE-derived and the observed SCO from the Dobson-ozonesonde measurements differ by more than 20 DU. During the rest of the year, the SAGE average is less than 2 DU lower than the measured SCO. Wang et al. did not discuss the seasonality of the differences because effects of synoptic scale differences tended to mask the effects of seasonality differences (D. M. Cunnold, personal communication, 2005).

[33] Without the empirical correction, Table 3a shows that the average monthly difference between the SBUV SCO derived from the version 6 archive and the measured SCO is 14 DU, nearly twice as large as the difference calculated using SAGE. Every month shows SBUV SCO integrals higher than the observations. On the other hand, with the empirical correction, the agreement between the EC-SBUV SCO and the measured SCO is comparable to the agreement between the SAGE and measured SCO.

[34] Table 3b and Figure 10b summarize the measurements at Wallops Island. The amplitude of the seasonal cycle is less than that at Hohenpeissenberg and is captured by all three data sets. As with Hohenpeissenberg, the four months of the greatest differences (>10 DU) between the SAGE and Dobson-ozonesonde SCO, (February, July, September, and November) all show higher SAGE amounts. Without the empirical correction, the SBUV integrals are significantly higher than both the measured and SAGE SCO values. With the correction, the EC-SBUV SCO is once

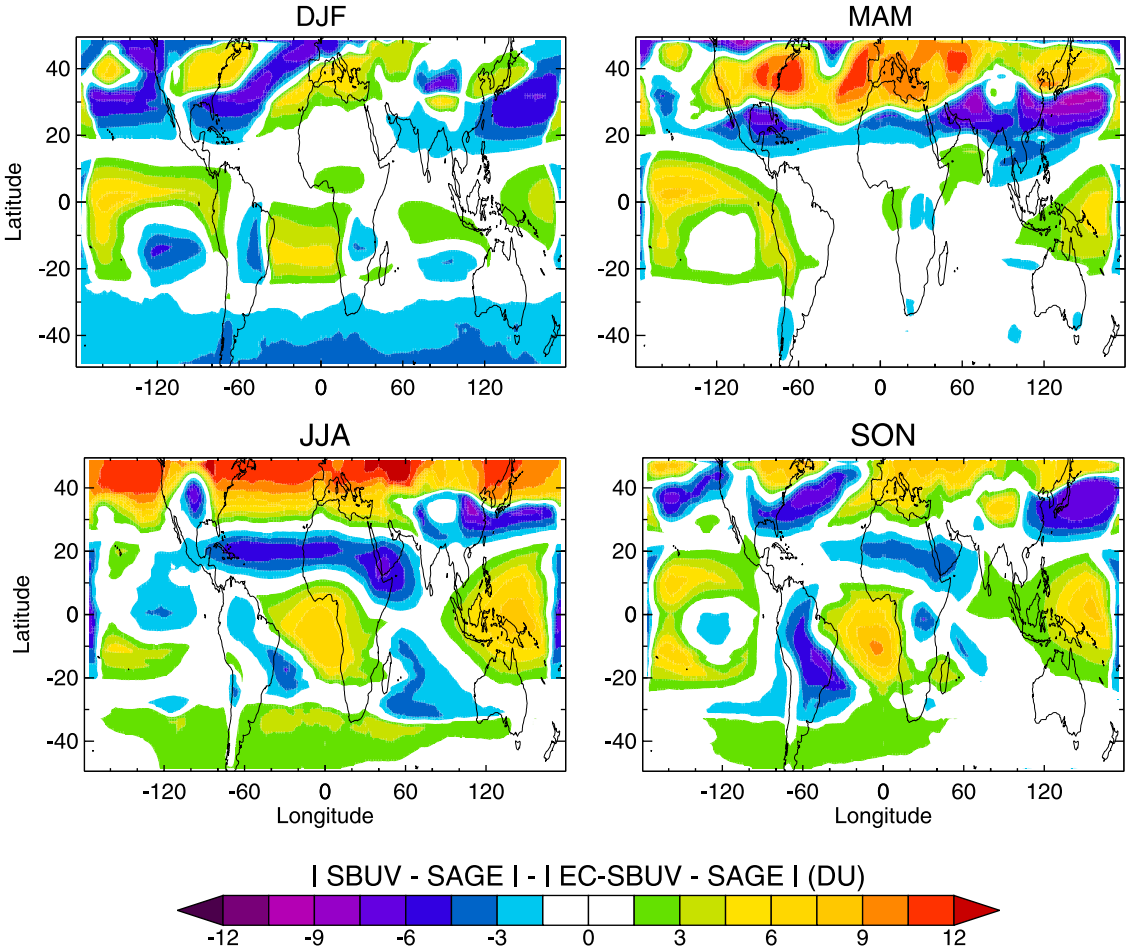

Figure 9. Distribution of |SBUV-SAGE| – |EC-SBUV-SAGE|. Regions with positive values show where the empirical correction has brought the SBUV fields closer to the stratospheric column ozone fields generated using SAGE measurements.

again slightly better than the agreement found between the observed SCO than the SAGE SCO values.

[35] Figure 11 shows monthly mean EC-SBUV SCO values compared with the ground-based/in situ SCO at the stations listed in Table 2. For each station, monthly EC-SBUV SCO values (open triangles) are plotted with monthly ozonesonde/ground-based SCO values (asterisks). Table 4 summarizes the impact of the empirical correction on the data shown in Figure 11 by comparing the corresponding monthly mean error, standard deviation, and root-mean square error, for the EC-SBUV in these plots with both the ground-based/in situ measurements and with the SCO

Table 3a. Seasonal Cycle of Observed SCO Over Hohenpeissenberg Compared With SCO Derived From Satellite Measurements[a]

Month	SCO[b]	SAGE	|Diff|	SBUV	|Diff|	EC-SBUV	|Diff|
Jan	302	307	5	306	4	301	1
Feb	321	311	10	329	8	323	2
March	338	342	4	339	1	331	7
April	338	338	0	350	12	340	2
May	324	322	2	343	19	330	6
June	307	294	13	327	20	314	7
July	291	285	6	307	16	294	3
Aug	278	276	2	292	14	282	4
Sept	258	264	6	277	19	266	8
Oct	254	256	2	267	13	258	4
Nov	251	272	21	268	17	259	8
Dec	268	290	22	288	20	282	14
Average	294	296	8	308	14	298	6

[a]All values given in Dobson Units.
[b]Dobson-Ozonesonde.

Table 3b. Seasonal Cycle of Observed SCO Over Wallops Island Compared With SCO Derived From Satellite Measurements[a]

Month	SCO[b]	SAGE	|Diff|	SBUV	|Diff|	EC-SBUV	|Diff|
Jan	285	280	5	290	5	285	0
Feb	286	304	18	301	15	293	7
March	304	303	1	314	10	306	1
April	308	310	2	320	12	308	0
May	293	299	6	313	20	300	7
June	285	281	4	294	9	282	3
July	264	274	10	279	15	271	7
Aug	258	259	1	272	14	267	9
Sept	246	257	11	263	17	257	11
Oct	250	257	7	259	9	253	3
Nov	244	258	14	256	12	249	5
Dec	268	262	6	272	4	266	2
Average	274	279	7	286	12	278	5

[a]All values given in Dobson Units.
[b]Dobson-Ozonesonde.

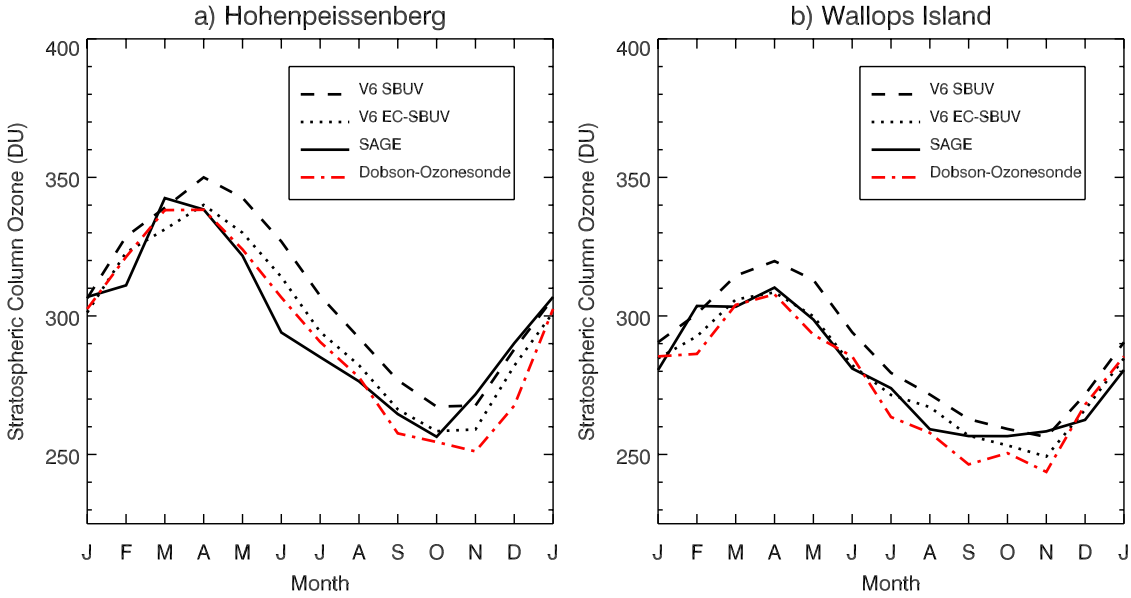

Figure 10. Seasonal cycle of SCO at Hohenpeissenberg, Germany, and Wallops Island, United States. The Dobson-ozonesonde values are plotted as thick dash-dotted (red) line; the satellite-derived (black) lines show SAGE SCO (thin solid line) and SBUV SCO (dashed line) and the EC-SBUV SCO (dotted line).

derived from the archived SBUV profiles (not plotted in Figure 11). We see from this table that the empirical correction has reduced the mean difference by an overall average of 4 DU. Thus, in addition to improvements at Hohenpeissenberg and Wallops Island described earlier, there is also better agreement of the EC-SBUV SCO with the ground-based/in situ SCO than the archived SBUV SCO at almost every station where enough ozonesonde data are available to perform such analyses.

6. Discussion

[36] It is generally agreed that stratospheric ozone distributions derived from SAGE, MLS and HALOE provide better vertical resolution than SBUV and that these datasets have undergone extensive validation [*WMO*, 1999]. The objective of this study is to show that the resultant SCO fields derived using SBUV data that have been modified by the empirical correction described by *Fishman et al.* [2003] provide a SCO dataset that is comparable in accuracy to one of these other instruments, SAGE. Validation of the TOR derived from the use of TOMS can be done only by comparing these derived data with measurements from only a handful of available ozonesonde sites. Such studies have already been performed. For example, we point to the detailed study by *Sun* [2002] that summarizes all published techniques prior to the EC-TOR data set described by *Fishman et al.* [2003].

[37] As an alternative to a direct validation of the TOR product that is derived from the empirical correction methodology, this study has concentrated on the robust stratospheric ozone data set from SBUV to provide additional insight into the accuracy of the resultant EC-TOR fields derived using these SCO fields in conjunction with coincident TOMS total ozone measurements. The SCO fields respond to large-scale forcing, and it is important that the large-scale features picked up by different instruments are consistent with validation measurements and with each other. If these facts are verifiable, then we can assume that the smaller scale variability, which is solely the result of the greater spatial resolution of TOMS, is, in fact, a true tropospheric feature.

[38] Unlike previous studies that look at TOR information only at low latitudes, this EC-TOR technique provides information at middle latitudes where there are considerably more SAGE and ozonesonde profiles. We have shown that the SCO derived from SBUV data after the empirical correction has been applied improves the amount of ozone in SBUV Layer 3 and also provides excellent agreement with the SCO derived from the SAGE data set. The regions of greatest difference between the SCO distributions derived from the two different data sets coincides with regions where the height of the tropopause is most difficult to define [*Fishman et al.*, 1990; *Pierce et al.*, 2003].

7. Summary and Conclusions

[39] We have completed an in-depth analysis of the distribution of stratospheric ozone using SBUV profile data that have been modified according to the "empirical correction" described by *Fishman et al.* [2003]. We have found the following: (1) The empirical correction improves the calculated SCO relative to the archived SBUV (version 6) profiles as compared to ozonesonde data; (2) at the limited number of stations for which long-term ozonesonde records exist, the SCO derived from the EC-SBUV data agree with the ozonesonde data as well as SCO derived from SAGE measurements; (3) over the 50°N–50°S domain for which a climatology has been derived, the SCO seasonal distributions using the EC-SBUV database are similar to those derived from SAGE measurements; and (4) regions where the SAGE and SBUV distributions differ the most are in locations where

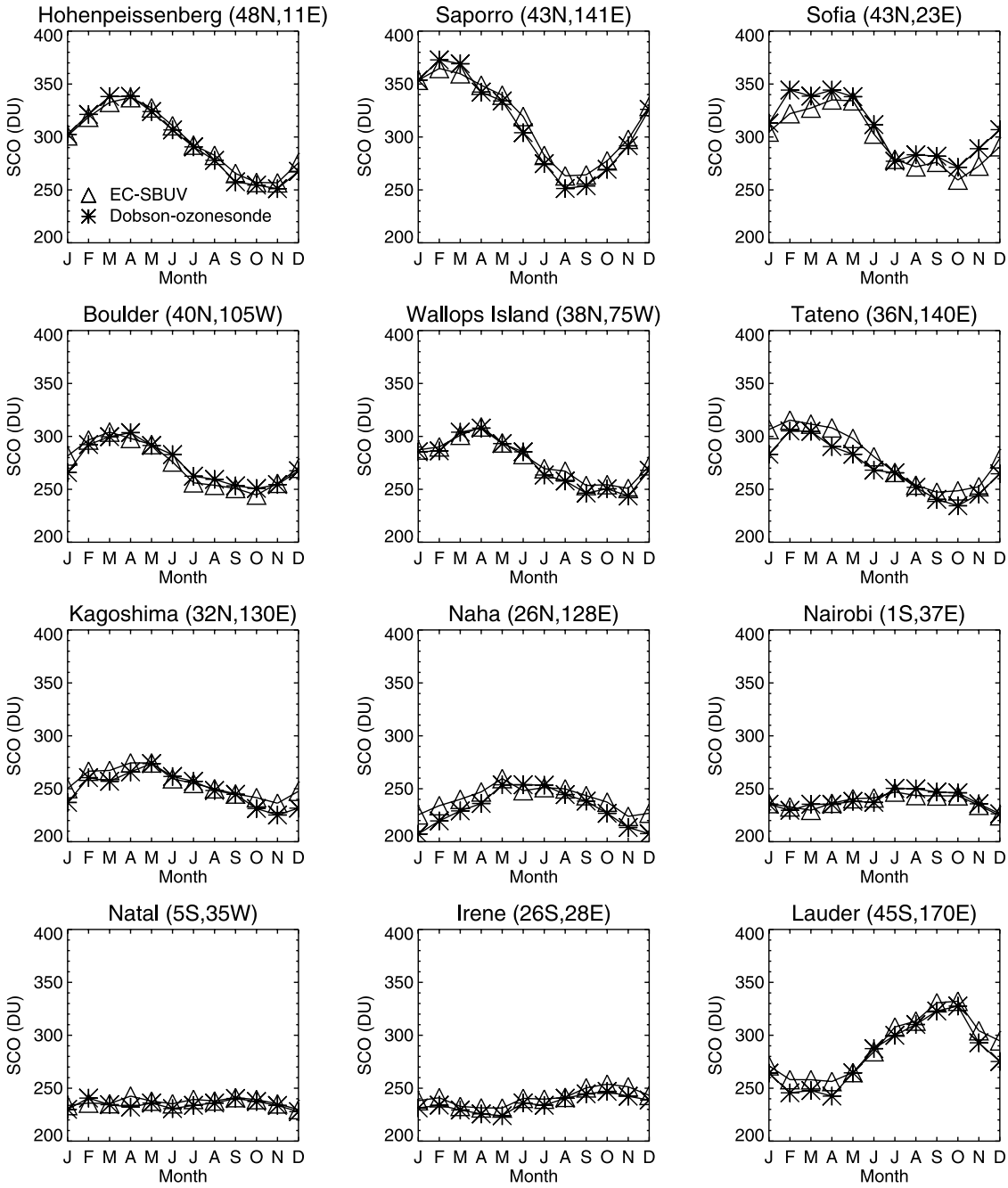

Figure 11. Monthly mean stratospheric column ozone derived from EC-SBUV and Dobson-ozonesonde measurements. The triangles are the EC-SBUV SCO and the asterisks are Dobson-ozonesonde SCO.

Table 4. Monthly Mean Error, Standard Deviation, and RMSE for Stratospheric Column Ozone[a]

	Empirically Corrected SBUV			SBUV From V6 Archive		
Station	ME	SDE	RMSE	ME	SDE	RMSE
Hohenpeissenberg, Germany	2.27	4.24	4.66	11.60	5.73	12.83
Sapporo, Japan	4.73	7.47	8.57	10.64	9.56	14.03
Sofia, Bulgaria	−10.35	6.31	11.98	−2.21	8.64	8.56
Boulder, Colorado	−0.33	6.63	6.35	9.60	5.95	11.16
Wallops Island, Virginia	3.33	3.82	4.94	11.20	2.59	11.47
Tateno, Japan	10.91	6.22	12.61	18.38	7.74	19.82
Kagoshima, Japan	6.17	7.45	8.58	12.75	6.68	14.27
Naha, Japan	8.61	8.61	11.18	13.03	8.29	15.26
Nairobi, Kenya	−1.12	3.46	3.50	1.24	1.71	2.05
Natal, Brazil	2.52	3.55	4.23	6.21	4.45	7.54
Irene, South Africa	5.60	2.10	5.95	7.78	2.49	8.14
Lauder, New Zealand	7.96	6.15	9.90	7.83	5.00	9.18

[a]All values given in Dobson Units.

strong jet stream activity is taking place, suggesting that neither can provide as accurate a data set as desired.

[40] The study by *Sun* [2002] has already provided a comprehensive analysis of the utility and the limitations for a number of studies that use a residual technique to infer tropospheric ozone from TOMS total ozone measurements. The EC-TOR data set described by *Fishman et al.* [2003] was not included in that analysis, but, in general, the same large-scale patterns seen by *Fishman et al.* [1990] and subsequent residual methods again show up in TOR depictions in the 2003 paper. The primary difference is the much higher spatial resolution highlighted in EC-TOR data, which is due to the much greater number of TOMS measurements used in the EC-TOR method.

Appendix A

[41] The primary rationale that prompted this study was to find an alternative methodology to validate the tropospheric ozone residual data set described by *Fishman et al.* [2003]. As pointed out by *Fishman* [2003], an interactive comment presented in response to *deLaat and Aben* [2003], there are no measurements available to validate the regional nature of elevated TOR amounts highlighted in the Fishman et al. paper. On the other hand, robust data sets do exist that can be used to validate the other quantity that must be generated to calculate the TOR, namely the SCO.

[42] During the course of our research, however, NOAA and NASA scientists were incorporating improvements into SBUV retrievals and eventually released version 8 of the data SBUV archive. The primary improvement in the version 8 algorithm is the incorporation of the *Logan* [1999] climatology as a priori information in the lowest three layers. Although the analysis of the SCO distribution would provide the most up-to-date comparison of how these fields compare with currently available ozonesonde and SAGE measurements, the SCO distributions derived with these more recently archived SBUV data would not be consistent with the data that went into the generation of the TOR fields discussed by *Fishman et al.* [2003].

[43] Furthermore, since the release of version 8 SBUV, only a handful of unpublished papers have been presented describing the accuracy of the data set [*McPeters et al.*, 2003; *Deland et al.*, 2004]. On the other hand, version 6 SBUV is a data set that has been used in numerous other studies and has been compared previously with other satellite measurements, as well as with ozonesonde measurements [e.g., *McPeters et al.*, 1994]. The additional analysis provided in the current study provides further insight into the shortcomings of the version 6 data set and proposes a method to remedy the observed problems, which were essentially implemented during the course of the current research and resulted in the release of version 8.

[44] We compared version 6 and version 8 SBUV ozone columns above 63 hPa derived from NIMBUS-7 (1979-1990) and NOAA-11 (1989–2000) measurements. For the NOAA-11 SBUV/2 data, (version 8–version 6) mean differences averaged over 10° latitude bands between 50°S and 50°N are approximately 1% (∼2DU). The 1-sigma standard deviation is approximately 2.5%. For the NIMBUS-7 SBUV data, which were used for less than one fourth of the SCO calculations in this study (1985–1989), mean differences averaged over 10° latitude bands between 50°S and 50°N are approximately 3% (∼6 DU). The 1-sigma standard deviation is approximately 3%. The correlation between version 6 and version 8 column ozone above 63 hPa is greater than 0.90 for each year of data. In our comparison of SBUV SCO with SAGE, The EC-SBUV profiles should be an excellent approximation of the version 8 SBUV profiles, particularly for the NOAA-11 instrument data.

[45] Finally, a companion paper, *Fishman et al.* [2005], discusses the interannual variability (IAV) of the SCO fields discussed in this paper and the regional nature of IAV found in the corresponding TOR data set. The *Fishman et al.* [2005] study provides additional credibility to the SCO derived in the present study by showing that these data are consistent with previous stratospheric ozone IAV studies that have used TOMS total ozone and SAGE ozone profile measurements to provide insight into the relationship between the quasi-biennial oscillation and the dynamics that impact the distribution of stratospheric ozone.

[46] **Acknowledgments.** SBUV/2 data were obtained from NOAA/NESDIS with support from the NOAA Climate and Global Change Program Atmospheric Chemistry Element. We thank T. Zenker for his work on the vertical interpolation of the SBUV data and V. Brackett for maintaining the ozonesonde database. We also thank Gary Morris and the anonymous referees whose comments greatly improved the manuscript.

References

Beekman, M., et al. (1997), Regional and global tropopause fold occurrence and related ozone flux across the tropopause, *J. Atmos. Chem.*, *28*, 29–44.

Bhartia, P. K., R. D. McPeters, C. L. Mateer, L. E. Flynn, and C. Wellemeyer (1996), Algorithm for the estimation of vertical ozone profiles from the backscatter ultraviolet technique, *J. Geophys. Res.*, *101*, 18,793–18,806.

Bremer, H., et al. (2004), Spatial and temporal variation of MOPPITT CO in Africa and South America: A comparison with SHADOZ ozone and MODIS aerosol, *J. Geophys. Res.*, *109*, D12304, doi:10.1029/2003JD004234.

Chatfield, R. B., and H. Harrison (1977), Tropospheric ozone: 2. Variations along a meridional band, *J. Geophys. Res.*, *82*, 5969–5976.

Crutzen, P. J. (1974), Photochemical reactions initiated by and influencing ozone in unpolluted tropospheric air, *Tellus*, *26*, 47–57.

deLaat, A. T. J., and I. Aben (2003), Problems regarding the tropospheric O3 residual method and its interpretation in Fishman et al. (2003), *Atmos. Chem. Phys. Discuss.*, *3*, 5777–5802.

Deland, M. T., et al. (2004), Long-term SBUV and SBUV/2 instrument calibration for version 8 ozone data, in *Proceedings of the XX Quadrennial Ozone Symposium, 1–8 June 2004, Kos, Greece*, edited by C. S. Zerefos, pp. 321–322, Univ. of Athens, Athens, Greece.

Diab, R. D., A. M. Thompson, K. Mari, L. Ramsay, and G. J. R. Coetzee (2004), Tropospheric ozone climatology over Irene, South Africa, from 1990 to 1994 and 1998 to 2002, *J. Geophys. Res.*, *109*, D20301, doi:10.1029/2004JD004793.

Fabian, P., and P. G. Pruchniewicz (1973), Meridional distribution of tropospheric ozone from ground-based registrations between Norway and South Africa, *Pure Appl. Geophys.*, *106*(5–7), 1027–1035.

Fabian, P., and P. G. Pruchniewicz (1977), Meridional distribution of ozone in the troposphere and its seasonal variations, *J. Geophys. Res.*, *82*, 2063–2073.

Fioletov, V. E., J. B. Kerr, E. W. Hare, G. J. Labow, and R. D. McPeters (1999), An assessment of the world ground-based total ozone network performance from the comparison with satellite data, *J. Geophys. Res.*, *104*, 1737–1747.

Fishman, J. (2003), Interactive comment on "Problems regarding the O_3 residual method and its interpretation in Fishman et al. (2003)" by A. T. J. deLaat and I. Aben, Atmos. Chem. Phys. Discuss., 3, S2208-S2215. (Available at http://www.atmos-chem-phys.org/adpd/3/S2208)

Fishman, J., and A. E. Balok (1999), Calculation of daily tropospheric ozone residuals using TOMS and empirically improved SBUV measurements: Application to an ozone pollution episode over the eastern United States, *J. Geophys. Res.*, *104*, 30,319–30,340.

Fishman, J., and P. J. Crutzen (1978), The origin of ozone in the troposphere, *Nature*, *274*, 855–858.

Fishman, J., S. Solomon, and P. J. Crutzen (1979), Observational and theoretical evidence in support of a significant in-situ photochemical source of tropospheric ozone, *Tellus*, *31*, 432–446.

Fishman, J., C. E. Watson, J. C. Larsen, and J. A. Logan (1990), Distribution of tropospheric ozone determined from satellite data, *J. Geophys. Res.*, *95*, 3599–3617.

Fishman, J., V. G. Brackett, E. V. Browell, and W. B. Grant (1996a), Tropospheric ozone derived from TOMS/SBUV measurements during TRACE-A, *J. Geophys. Res.*, *101*, 24,069–24,082.

Fishman, J., J. M. Hoell Jr., R. D. Bendura, R. J. McNeal, and V. W. J. H. Kirchoff (1996b), NASA GTE TRACE-A experiment (September–October 1992): Overview, *J. Geophys. Res.*, *101*, 23,865–23,879.

Fishman, J., A. E. Wozniak, and J. K. Creilson (2003), Global distribution of tropospheric ozone from satellite measurements using the empirically corrected tropospheric ozone residual technique: Identification of the regional aspects of air pollution, *Atmos. Chem. Phys.*, *3*, 893–907.

Fishman, J., J. K. Creilson, A. E. Wozniak, and P. J. Crutzen (2005), Interannual variability of stratospheric and tropospheric ozone determined from satellite measurements, *J. Geophys. Res.*, *110*, D20306, doi:10.1029/2005JD005868.

Hudson, R. D., and A. M. Thompson (1998), Tropical tropospheric ozone from Total Ozone Mapping Spectrometer by a modified residual method, *J. Geophys Res.*, *103*, 22,129–22,145.

Kaye, J. A., and J. Fishman (2003), Stratospheric ozone observations, in *Handbook of Climate, Weather, and Water: Chemistry, Impacts, and Applications*, edited by T. D. Potter and B. Colman, pp. 385–404, John Wiley, Hoboken, N. J.

Logan, J. A. (1985), Tropospheric ozone: Seasonal behavior, trends and anthropogenic influence, *J. Geophys. Res.*, *90*, 10,463–10,482.

Logan, J. A. (1999), An analysis of ozonesonde data for the troposphere: Recommendations for testing 3-D models, and development of a gridded climatology for tropospheric ozone, *J. Geophys. Res.*, *104*, 16,115–16,149.

McPeters, R. D., D. F. Heath, and P. K. Bhartia (1986), Average ozone profiles for 1979 from the NIMBUS 7 SBUV instrument, *Geophys. Res. Lett.*, *13*, 1213–1216.

McPeters, R. D., T. Miles, L. E. Flynn, C. G. Wellemeyer, and J. M. Zawodny (1994), Comparison of SBUV and SAGE II ozone profiles: Implications for ozone trends, *J. Geophys. Res.*, *99*, 20,513–20,524.

McPeters, R. D., et al. (2003), Ozone climatological profiles for version 8 TOMS and SBUV retrievals, *Eos Trans. AGU*, *84*(46), Fall Meet. Suppl., Abstract A21D-0998.

Newchurch, M. J., X. Liu, and J. H. Kim (2001), Lower-tropospheric ozone (LTO) derived from TOMS near mountainous regions, *J. Geophys. Res.*, *106*, 20,403–20,412.

Newchurch, M. J., D. Sun, J. H. Kim, and X. Liu (2003), Tropical tropospheric ozone derived using clear-cloudy pairs (CCP) of TOMS measurements, *Atmos. Chem. Phys.*, *3*, 683–695.

Pierce, R. B., et al. (2003), The Regional Air Quality Modeling System (RAQMS) predictions of the tropospheric ozone budget over east Asia, *J. Geophys. Res.*, *108*(D21), 8825, doi:10.1029/2002JD003176.

Prinn, R. G. (1988), Toward an improved network for determination of tropospheric ozone climatology and trend, *J. Atmos. Chem.*, *6*, 281–298.

SPARC (1998), Assessment of trends in the vertical distribution of ozone, *Rep. 43*, World Meteorol. Org. Global Ozone Res. and Monit. Project, Geneva.

Sun, D. (2002), Tropical tropospheric ozone: New methods, comparisons, and model evaluation of controlling processes, dissertation, 174 pp., Dep. of Atmos. Sci., Univ. of Ala., Huntsville.

Thompson, A. M., et al. (2003), Southern Hemisphere Additional Ozonesondes (SHADOZ) 1998–2000 tropical ozone climatology: 2. Tropospheric variability and the zonal wave-one, *J. Geophys. Res.*, *108*(D2), 8241, doi:10.1029/2002JD002241.

Vukovich, F. M., V. Brackett, J. Fishman, and J. E. Sickles II (1996), On the feasibility of using the tropospheric ozone residual for nonclimatological studies on a quasi-global scale, *J. Geophys. Res.*, *101*, 9093–9105.

Vukovich, F. M., V. Brackett, J. Fishman, and J. E. Sickles II (1997), A 5-year evaluation of the tropospheric ozone residual at nonclimatological periods, *J. Geophys. Res.*, *102*, 15,927–15,932.

Wang, H. J., D. M. Cunnold, L. W. Thomason, J. M. Zawodny, and G. E. Bodeker (2002), Assessment of SAGE version 6.1 ozone data quality, *J. Geophys. Res.*, *107*(D23), 4691, doi:10.1029/2002JD002418.

Wang, Y. H., J. A. Logan, and D. J. Jacobs (1998), Global simulation of O-3-NOx-hydrocarbon chemistry: 3. Origin of tropospheric ozone and effects of non-methane hydrocarbon, *J. Geophys. Res.*, *103*, 10,757–10,767.

World Meteorological Organization (1999), Scientific assessment of ozone depletion: 1998, *Rep. 44*, 732 pp., Global Ozone Res. and Monit. Project, Geneva.

World Meteorological Organization (2003), Scientific assessment of ozone depletion: 2002, *Rep. 47*, 498 pp., Global Ozone Res. and Monit. Project, Geneva.

Ziemke, J. R., S. Chandra, and P. K. Bhartia (1998), Two new methods for deriving tropospheric column ozone from TOMS measurements: Assimilated UARS MLS/Haloe and convective-cloud differential techniques, *J. Geophys. Res.*, *103*, 22,115–22,127.

J. K. Creilson and J. Fishman, NASA Langley Research Center, Mail Stop 401A, Hampton, VA 23681, USA. (j.k.creilson@larc.nasa.gov; jack.fishman@nasa.gov)

P.-H. Wang, NASA Langley Research Center, Mail Stop 910, Hampton, VA 23681, USA. (p.wang@larc.nasa.gov)

A. E. Wozniak, NASA Goddard Space Flight Center, Code 613.3, Greenbelt, MD 20771, USA. (a.e.wozniak@larc.nasa.gov)